



Shear wave splitting and the pattern of mantle flow beneath eastern Oregon

Maureen D. Long ^{a,*}, Haiying Gao ^b, Amanda Klaus ^{c,1}, Lara S. Wagner ^d, Matthew J. Fouch ^e, David E. James ^f, Eugene Humphreys ^b

^a Department of Geology and Geophysics, Yale University, New Haven, CT, USA

^b Department of Geological Sciences, University of Oregon, Eugene, OR, USA

^c Scripps College, Claremont, CA, USA

^d Department of Geological Sciences, University of North Carolina, Chapel Hill, NC, USA

^e School of Earth and Space Exploration, Arizona State University, Tempe, AZ, USA

^f Department of Terrestrial Magnetism, Carnegie Institution of Washington, Washington DC, USA

ARTICLE INFO

Article history:

Received 7 April 2009

Received in revised form 11 September 2009

Accepted 26 September 2009

Available online 29 October 2009

Editor: Y. Ricard

Keywords:

intraplate volcanism

High Lava Plains

Blue Mountains

Pacific Northwest

mantle flow

shear wave splitting

seismic anisotropy

ABSTRACT

The tectonic and geologic setting of eastern Oregon includes the volcanically active High Lava Plains (HLP) province and the accreted terrains of the Blue and Wallowa Mountains and is bounded by the Columbia River flood basalts to the north, Basin and Range extension to the south, the Cascade arc to the west, and stable North America to the east. Several models have been proposed to explain the tectonic evolution of eastern Oregon and, in particular, the voluminous volcanic activity in the HLP, but a consensus on which model fully describes the complex range of processes remains elusive. Measurements of the seismic anisotropy that results from active mantle flow beneath the region can provide a crucial test of such models. To constrain this anisotropy, here we present new SKS splitting results obtained at approximately 200 broadband seismic stations in eastern Oregon and the surrounding region. Data come from the USArray Transportable Array (TA) and two temporary experiments carried out in the HLP and in the Wallowa Mountains. Our splitting data set includes ~2900 individual splitting measurements from SKS phases recorded between 2006 and 2008. Stations in eastern Oregon exhibit significant shear wave splitting, with average delay times at individual stations between ~0.8 s and ~2.7 s. In the HLP, nearly all observed fast directions are approximately E-W, while to the north in the Blue and Wallowa Mountains there is more variability in the splitting patterns. The average delay time observed at stations located in the heart of the HLP province is ~2 s, well above the global average of ~1 s for continental regions. We infer from the large split times and homogeneous fast directions that there must be significant active flow in a roughly E-W direction in the asthenosphere beneath the HLP; this inferred flow field places a strong constraint on models that seek to explain the young tectonomagmatic activity in the region. In the Wallowa region, the anisotropic signature is more complicated and there may be a significant contribution from fossil fabrics in the crust or mantle lithosphere.

© 2009 Elsevier B.V. All rights reserved.

1. Introduction

Varied tectonic and geological terranes comprise the Cascadian backarc of eastern Oregon, including the volcanically active High Lava Plains (HLP) and the older Mesozoic accreted terranes of the Blue and Wallowa Mountains. The region is bounded by the Columbia River Basalt group to the north, the arc volcanoes of the Cascades to the west, and Precambrian North America to the east, and it transitions into extensional Basin and Range to the south (Fig. 1). The region's recent geological history is dominated by voluminous intraplate

magmatism, with the appearance of the Columbia River and Steens flood basalts along the western margin of the North American craton at ~17–15 Ma followed by a still ongoing period of bimodal (basaltic and silicic) volcanism in both the High Lava Plains and Snake River Plain to the east. The causes of this ongoing tectonomagmatic activity and its relationship to other tectonic processes, such as the uplift of the Wallowa Mountains in northeastern Oregon, are not well understood. A variety of models for the widespread volcanism has been proposed, which variously invoke the inferred Yellowstone plume (e.g., Camp and Ross, 2004), rollback and steepening of the Cascadia slab (e.g., Carlson and Hart, 1987), lithospheric extension related to the Basin and Range to the south (e.g., Cross and Pilger, 1978), localized lithospheric delamination (Hales et al., 2005), or a combination of these processes. A consensus on which model best explains the current range of geological, geochemical, petrological, and geophysical data, however, has not been forthcoming.

* Corresponding author.

E-mail address: maureen.long@yale.edu (M.D. Long).

¹ Now at: Department of Earth and Space Sciences, University of Washington, Seattle, WA, USA.

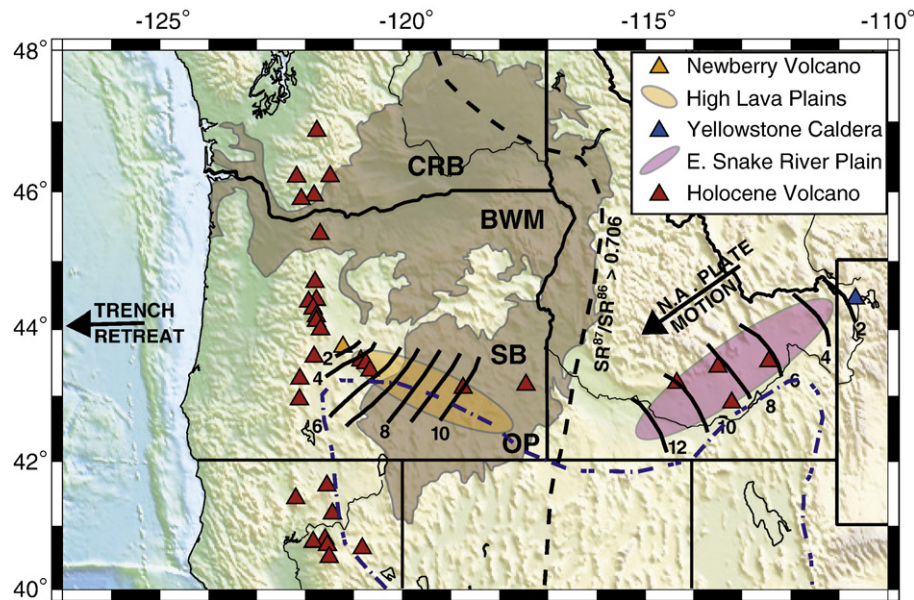


Fig. 1. Geologic map of eastern Oregon and the surrounding region. Black contours indicate the age progression (in Ma) of silicic volcanism along both the High Lava Plains (Jordan et al., 2004), shown in yellow, and the Snake River Plain (Christiansen et al., 2002), shown in pink. The black dashed line shows the location of the $Sr^{87}/Sr^{86} = 0.706$ line (after Jordan et al., 2004, using data from Leeman et al., 1992), commonly interpreted to mark the boundary between cratonic North America to the east and the accreted arc terranes to the west. The blue dashed line shows the northern limits of Basin and Range extension (e.g., Wernicke et al., 1988). The brown highlighted area indicates the region covered by Miocene flood basalts (Camp and Ross, 2004), including the Columbia River basalts (CRB) to the north and the Steens basalts (SB) farther to the south. Red triangles indicate locations of Holocene volcanism. The geographical locations of the Owyhee Plateau (OP) and the Blue and Wallowa mountains (BWM) are also shown, along with Newberry Volcano (orange triangle) and Yellowstone Caldera (blue triangle). The arrow at the Cascadia trench indicates its direction of motion; the trench is retreating at a rate of ~ 30 mm/yr in a Pacific hotspot reference frame (Schellart et al., 2008).

One important discriminant among the many models that have been proposed for the tectonic evolution of eastern Oregon is the geometry of upper mantle flow. Constraints on this mantle flow can be inferred from measurements of elastic anisotropy, which manifests itself in the seismic wavefield in several different ways. In the upper mantle, seismic anisotropy is generally ascribed to the crystallographic or lattice preferred orientation (LPO) of individual mineral crystals (primarily olivine) that are themselves anisotropic (e.g., Karato et al., 2008). When a volume of mantle rock is subjected to strain under dislocation creep conditions, it develops an LPO, and the resulting anisotropy can be measured using seismological techniques. Anisotropy resulting from shape preferred orientation of partial melt lenses (e.g., Zimmerman et al., 1999) may also be important beneath the HLP, particularly given the evidence of high uppermost mantle temperatures in that region (e.g., Warren et al., 2008). The measurement of the splitting or birefringence of seismic shear waves (particularly core-refracted phases such as SKS) represents one of the most direct ways to probe anisotropy in the upper mantle (for overviews, see Silver, 1996; Savage, 1999; Fouch and Rondenay, 2006; Long and Silver, 2009). However, because splitting is a path-integrated measurement, anisotropy anywhere along the receiver side of the SKS raypath will contribute to the observed splitting and in practice this means that the depth resolution of splitting measurements is poor. In particular, in continental settings it can be difficult to distinguish between lithospheric anisotropy that developed as a consequence of past deformational processes and anisotropy in the asthenosphere that is associated with active mantle flow. Despite these difficulties, however, splitting measurements when properly interpreted can yield tight constraints on the geometry of mantle flow beneath a seismic station, and can help to distinguish among different models for past and ongoing tectonic processes.

In this study we present measurements of SKS splitting at 200 broadband stations in eastern Oregon and the surrounding regions (central Oregon, western Idaho, northern Nevada, and southeastern Washington). The goal of this effort is not only to characterize SKS splitting using an extremely dense broadband array, but also to use

these measurements and other geophysical observations to distinguish between lithospheric and asthenospheric contributions to anisotropy and to characterize the pattern of active mantle flow beneath eastern Oregon. These inferences can then be placed in the context of the shear wave splitting pattern observed in the western United States (e.g., Zandt and Humphreys, 2008; Fouch and West, in preparation) and used to discriminate among the many models for the recent tectonic evolution of the region. In this paper, we focus on the presentation of the highest-quality measurements from the splitting data set in order to present a first-order picture of shear wave splitting, upper mantle anisotropy, and mantle flow beneath the region.

2. Tectonic, geologic, and geophysical setting

The western United States in general and the region surrounding Eastern Oregon in particular has a rich and complicated tectonic history (for a recent overview, see Humphreys and Coblenz, 2007). Extensive magmatic activity in eastern Oregon has been documented beginning in the Cenozoic, when the so-called “ignimbrite sweep” (e.g., Lipman et al., 1972) resulted in large-volume silicic magmatism over much of western North America between 50 and 20 Ma. Between 17 and 15 Ma, volcanic activity in the region was dominated by the massive flood basalt eruptions that began in the McDermitt area near the Oregon/Idaho/Nevada border with the Steens basaltic volcanism. Following the Steens event, flood volcanism propagated northward along the western edge of Precambrian North America, culminating in the voluminous outpourings of Columbia River basalts. Since approximately 14–12 Ma, volcanic activity in eastern Oregon has been dominated by major eruptions along the temporally migrating volcanic track of the High Lava Plains that extends from southeastern Oregon northwest to Newberry volcano in the Cascades (Fig. 1). In an almost mirror image, the considerably more voluminous Yellowstone-Snake River Plain (YSRP) volcanism followed a contemporaneous migration northeastward from the McDermitt caldera area in northern Nevada to Yellowstone in Montana, producing a prominent volcanic

lineament that has been widely interpreted as corresponding to the trace of the Yellowstone hot spot track (e.g., [Pierce and Morgan, 1992](#)). For both HLP and YSRP, the volcanism is characterized by bimodal silicic and basaltic eruptions. In the HLP, the silicic volcanism exhibits an age progression from southeast to northwest that has been documented using $^{40}\text{Ar}/^{39}\text{Ar}$ dating ([Jordan et al., 2004](#)), but basaltic volcanic activity has been widespread and there are Holocene basalt flows in disparate locations ([Fig. 1](#)). To the north of the HLP, the Blue and Wallowa mountains are composed of older Mesozoic accreted terranes; the Wallowas in particular underwent significant uplift during and after the Columbia River basalt eruptions ([Hales et al., 2005](#)).

A variety of models has been proposed to explain the formation of the High Lava Plains and the tectonic evolution of eastern Oregon. A primary question is whether or not it is necessary to invoke a mantle plume to explain HLP volcanism. Models that invoke a plume as the origin for both the Columbia River/Steens flood basalts and the HLP/YSRP volcanic trend have been proposed (e.g., [Camp and Ross, 2004](#)), but the role of a mantle plume in northwestern US volcanism continues to be hotly debated (e.g., [Humphreys et al., 2000](#); [Jordan, 2005](#); [Hooper et al., 2007](#)). Alternative models invoke asthenospheric inflow due to the rollback and steepening of the Cascadia slab ([Carlson and Hart, 1987](#)), significant lithospheric extension associated with the external Basin and Range to the south ([Cross and Pilger, 1978](#)), or backarc spreading processes (e.g., [Christiansen and McKee, 1978](#); [Smith, 1992](#)). It remains unclear what role “topography” at the base of the lithosphere may have played in shaping the evolution of the HLP: for example, [Jordan et al. \(2004\)](#) suggested that buoyant plume material may have been guided along the thinning lithosphere to the northwest beneath the HLP, although lithospheric basal topography may play an equally important role in non-plume models as well. It has also been suggested that lithospheric delamination processes may have played a role in the tectonic evolution of eastern Oregon: [Hales et al. \(2005\)](#) proposed a delamination model to explain the location and timing of both the Columbia River basalt eruptions and the significant uplift (~2 km) of the Wallowa mountains. A consensus about which process (or combination of processes) is responsible for the volcanic and tectonic evolution of eastern Oregon has not yet been reached, but a detailed examination of shear wave splitting patterns in the region provides a promising way to discriminate among the many models because these models make substantially different predictions about contemporary flow processes in the upper mantle. For example, a plume model (e.g., [Camp and Ross, 2004](#)) would predict mantle flow radiating out from the presumed plume head location in southeastern Oregon, with flow along the strike of the HLP trend, while a model that invokes slab rollback and steepening (e.g., [Carlson and Hart, 1987](#)) would predict mantle flow in the direction of trench migration.

In addition to shear wave splitting, other geophysical observations can be brought to bear in order to discriminate among the different models. For example, new tomographic images of isotropic wave-speed velocities are yielding insight into mantle structure beneath the region. Several tomographic models for the western US have recently been published (e.g., [Burdick et al., 2008](#); [Roth et al., 2008](#); [Sigloch et al., 2008](#)) that provide an unprecedented level of detail. In particular, [Roth et al. \(2008\)](#) imaged several striking structural features in the upper mantle beneath the region, including an increased-velocity anomaly that is interpreted to be the Juan de Fuca slab, pronounced reduced-velocity anomalies beneath Newberry volcano, north-central Oregon, and (especially) the YSRP, reduced velocities in the uppermost mantle (~50–125 km depth) beneath the HLP, and increased velocities extending deep into the upper mantle beneath the Blue Mountains. The present-day crustal deformation field can also be used to discriminate among models for the tectonic evolution of eastern Oregon; crustal deformation has been studied in this region using GPS (e.g., [McCaffrey et al., 2000, 2007](#)). Block models that have

been produced to match the GPS observations indicate that eastern Oregon is currently undergoing rigid rotation about a pole located in northeastern Oregon or Idaho, with very little present-day crustal strain ([McCaffrey et al., 2007](#)).

3. Data and methods

Data from three different broadband seismic experiments are used in this study; a station map is shown in [Fig. 2](#). First, we utilize data from the Transportable Array (TA) seismic component of USArray, which will eventually cover the entire continental United States with an average station spacing of ~70 km. We present measurements for TA rows E (which covers southern Washington state and northern Idaho) through M (which covers northern California and northern Nevada), and TA columns 05–11 (that is, E05–E11, F05–F11, etc., through M05–M11), for a total of 62 stations. TA stations in this region were generally installed between late 2005 and mid-2006 and demobilized in mid- to late 2008. Second, the High Lava Plains (HLP) seismic experiment consists of an array of 118 broadband instruments, with a maximum of 104 currently operating (as of late 2008). The first stations in the HLP array were installed in early 2006; the bulk of the array was installed in mid-2007. The HLP station configuration consists of two dense lines, one of which stretches from the eastern Owyhee Plateau in southwest Idaho to Bend, Oregon ([Fig. 2](#)) and follows the spatiotemporal trend in the silicic volcanism ([Jordan et al., 2004](#)). The second line is aligned N-S and is designed to probe the transition from (south to north) Basin and Range extension to High Lava Plains volcanism to the accreted terranes of the Blue Mountains. The average station spacing along the dense lines is ~15–20 km and they are surrounded by “clouds” of stations with sparser spatial coverage. The third source of data is the Wallowa Mountains experiment, which began in Fall 2006. This experiment consists of an initial deployment of 20 stations around the Wallowa Mountains; in

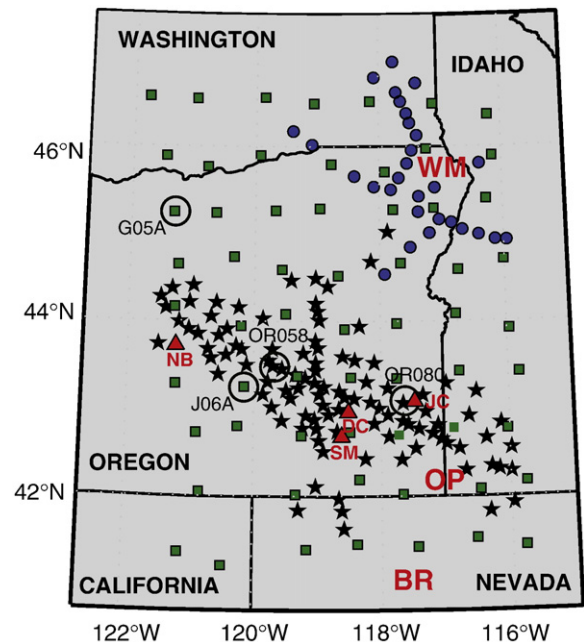


Fig. 2. Map of stations used in this study, including those from the Transportable Array (TA) (squares), the Wallowa Array (circles), and the High Lava Plains (HLP) array (stars). State names are shown and geographical features are marked for reference: the Basin and Range (BR), the Owyhee Plateau (OP), and the Wallowa Mountains (WM). Newberry Volcano (NB), Diamond Craters (DC), Jordan Craters (JC), Steens Mountain (SM), are all marked with red triangles. Four stations (G05A, J06A, OR058, and OR080) that are referred to by name in the paper are labeled.

May 2008 10 instruments were moved to create a 30-station array. The stations extend across the Precambrian continental margin to the east and north of the Willowa Mountains and also sample the transition across the old oceanic embayment to the northwest. Together, these three deployments provide extremely dense spatial sampling of eastern Oregon and the surrounding regions.

The measurements presented here resulted from a data processing effort involving the visual inspection of approximately 35,000 waveforms for data covering the period between January 2006 and October 2008. The splitting measurements were carried out using the SplitLab software package (Wüstefeld et al., 2007). We selected events of magnitude $M_w \geq 5.8$ located at epicentral distances between 88° and 130° for processing. An event map is shown in Fig. 3, along with a circular histogram showing the backazimuthal coverage in the

dataset. We note that the backazimuthal coverage for SKS phases in eastern Oregon is not ideal and is heavily weighted towards events in the western Pacific Ocean, which precludes a complete analysis of backazimuthal dependence of splitting parameters. We initially applied a bandpass filter to retain energy at periods between 10 and 100s and the horizontal components of the SKS waveform were examined for high signal-to-noise ratio and good waveform clarity. In approximately 20% of cases, the corner periods on the filter were adjusted slightly to optimize signal-to-noise ratio, such that energy at periods between 8 and 12s and 50 and 100s was retained. We then manually windowed around the SKS phase, selecting a window length that covers at least one full period of the signal. For several HLP stations, we experimented with different window lengths and found that varying the window length had a negligible effect on the measurements, particularly for the highest-quality measurements in the dataset.

We used both the cross-correlation and the transverse component minimization methods to identify the best-fitting splitting parameters (fast polarization direction ϕ and delay time δt) and only retained those measurements for which the 95% confidence regions using the two methods overlap. It has been shown that the two measurement methods can disagree for noisy data, complex anisotropic structure, or when the incoming polarization azimuth is close to the null direction (e.g., Long and van der Hilst, 2005; Wüstefeld and Bokelmann, 2007). Those few measurements which yielded well-constrained but discrepant splitting parameters from high-quality non-null waveforms using the different methods are not presented here, as the goal of this study is to identify the highest-quality splitting measurements at each station. We are mindful, however, that discrepancies among measurement methods may be due to complex anisotropy beneath the station, discussed further in Section 5. These measurements likely warrant further investigation in a future study. For the vast majority of the measurements in the dataset, however, potential biases introduced by the choice of measurement methods should be minimal, as previous studies have shown that different measurement methods yield similar results when applied to high-quality data in the presence of a single layer of horizontal anisotropy (Long and van der Hilst, 2005).

We identified as “good” those splitting measurements for which the signal-to-noise ratio and waveform clarity were high, the initial particle motion was elliptical, the corrected particle motion was linear or very nearly linear, the cross-correlation and transverse component minimization methods yielded splitting parameter estimates that were consistent within the errors, and the 2σ error spaces for each measurement were nearly elliptically shaped and small, with errors less than $\pm 15^\circ$ in fast direction and ± 0.3 s in delay time. Measurements with larger error bars (up to $\pm 30^\circ$ in ϕ and ± 1 s in δt) and lower signal-to-noise ratios (down to ~ 2 – 3) were marked as “fair” but were retained as long as the measurement methods agreed. Null measurements were identified by the initial linear particle motion and were also classified as “good” or “fair,” with noisier measurements classified as “fair.” An example of a high-quality splitting measurement is shown in Fig. 4.

4. Results

The splitting measurement procedure described above yielded a total of ~ 1950 well-constrained measurements of $(\phi, \delta t)$ at eastern Oregon stations. Of these, ~ 680 were classified as “good” and ~ 1270 as “fair.” In addition to these, ~ 950 high-quality (“good” + “fair”) null measurements were identified. Some individual stations had as many as 10–15 “good” quality measurements, while others had only a few and at several stations the measurement procedure only yielded “fair” quality measurements. In this paper, we focus on presenting the highest-quality measurements at each station; that is, either all “good” measurements or, at stations which have none, all “fair”

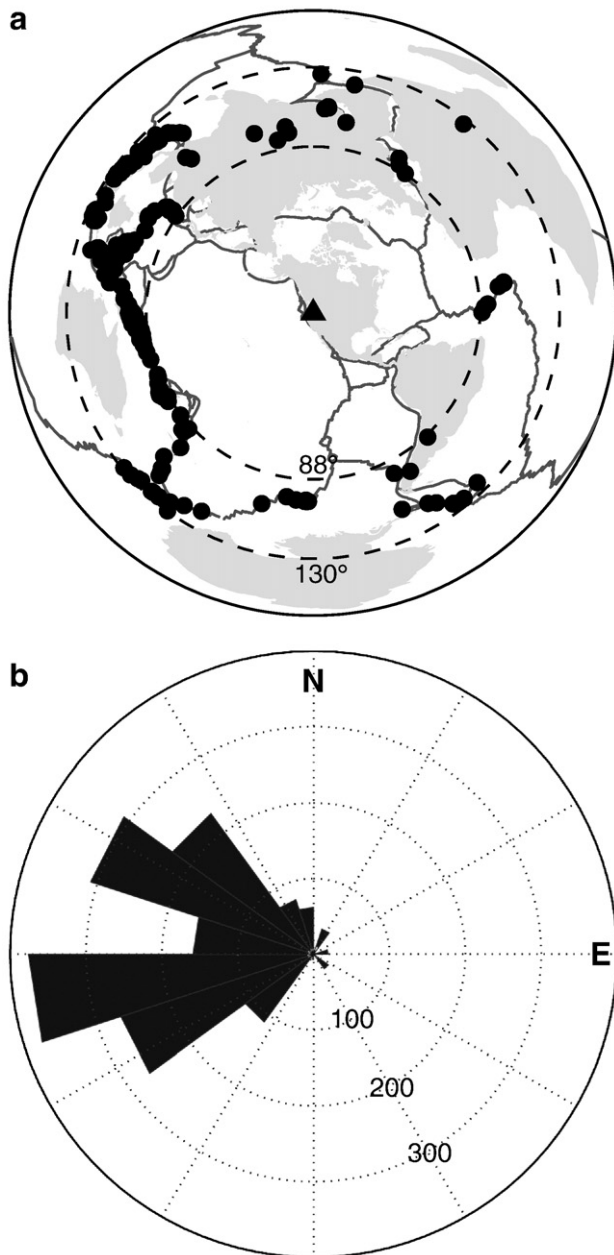


Fig. 3. a. Map of large-magnitude seismicity ($M \geq 5.8$) in the 88° – 130° epicentral distance range around a representative station (OR058; see Fig. 2) for the period 2006–2008. b. Circular histogram of event backazimuths for all “good” and “fair” quality measurements (null and non-null) in the data set; the backazimuthal coverage is heavily weighted towards events to the west.

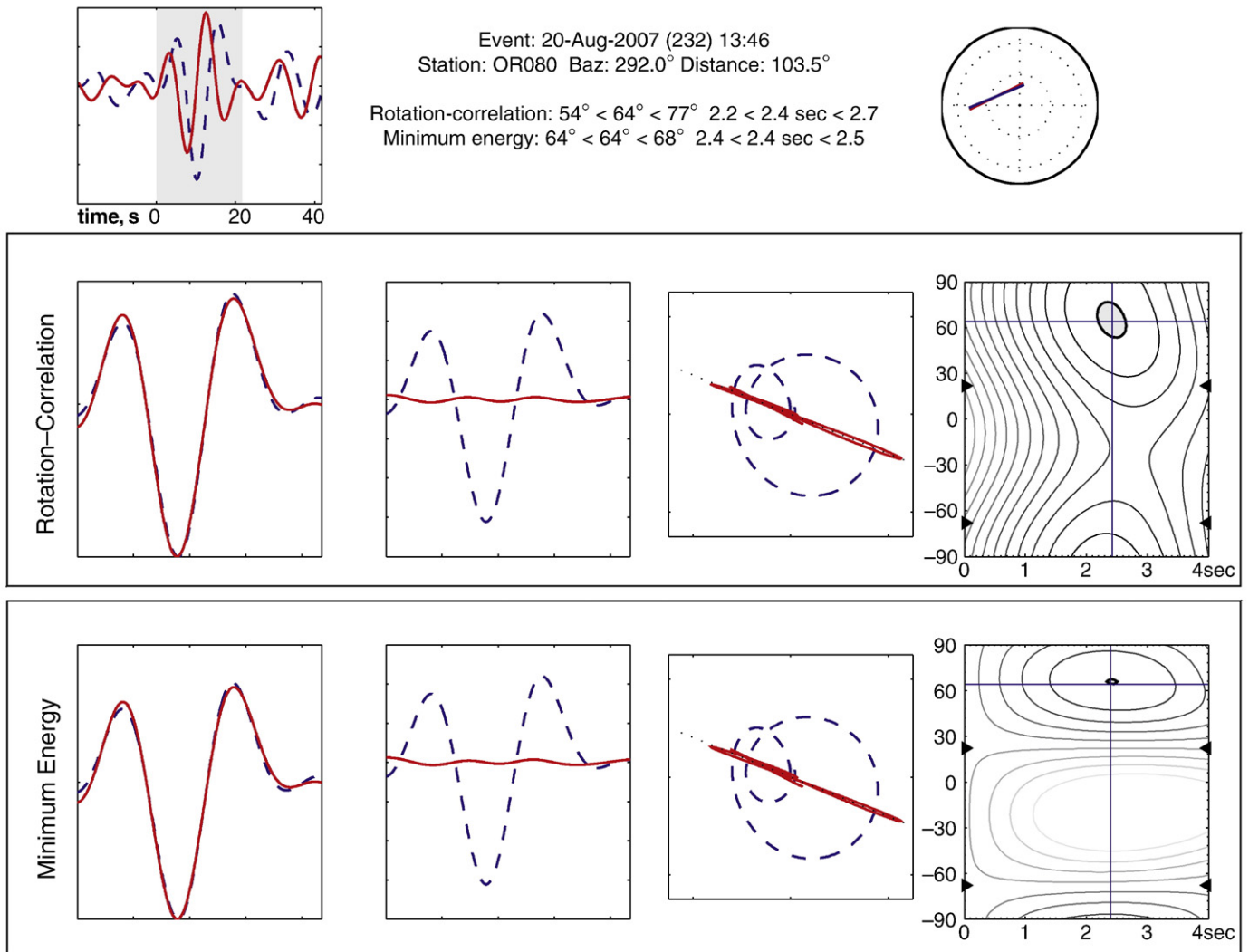


Fig. 4. An example of a high-quality (“good”) measurement at HLP station OR080 (see Fig. 2) obtained using SplitLab (Wüstefeld et al., 2007). Top left panel shows the uncorrected radial (blue dashed) and transverse (solid red) components; the time window used in the analysis is shown in gray. The middle and bottom rows of panels show the diagnostic plots for the rotation-correlation method and the transverse component minimization method, respectively: from left to right, the corrected fast and slow components, the corrected radial and transverse components, the uncorrected (blue dashed) and corrected (solid red) particle motion diagrams, and the error space maps. The gray region in the error space maps represents the 95% confidence ellipse. For the transverse component minimization method, this is calculated by assuming that the transverse component energy is χ^2 -distributed and estimating the number of degrees of freedom from the seismogram; for further details, see Silver and Chan (1991). For the rotation-correlation method, it is calculated using a Fisher transform approach; for further details, see Wüstefeld et al. (2007). Both methods yield well-constrained splitting parameters of $\phi = 64^\circ$, $\delta t = 2.4$ s, as shown in the plot at the top right.

measurements. A map showing the highest-quality individual splitting measurements at each station is shown in Fig. 5a, and a similar plot of all the well-constrained (“good” + “fair”) null measurements is shown in Fig. 5b.

Overall, splitting patterns beneath the region are fairly simple, with a few areas of localized complexity. At most stations, particularly the stations located in the southern part of the study area, the measured fast directions and delay times cluster closely around average values of $\sim N80^\circ E$ for ϕ and ~ 1.8 s for δt . There is somewhat more variation in the measured splitting parameters at individual stations located farther to the north in the Blue and Wallowa Mountain regions. At many of these stations, there is considerable scatter in the measured ϕ values, the delay times tend to be smaller than at stations to the south, and the backazimuthal spread in null measurements tends to be larger (Fig. 5b). Additionally, the waveforms themselves tend to be more complex at stations located in the northern part of the study region. In order to demonstrate this regional difference in splitting pattern complexity, we show in Fig. 6 the backazimuthal distribution of measured splitting parameters for a station located in the northern

part of the study area (G05A) and a station located in the HLP (J06A). The northern station exhibits significant variations in $(\phi, \delta t)$ with backazimuth and well-constrained nulls were identified over a large swath of backazimuths; such a pattern is consistent with complex anisotropic structure beneath the station (e.g., Silver and Savage, 1994), and the delay times indicate that the anisotropy is weaker than elsewhere in the study area. In contrast, the southern station exhibits very similar splitting over a wide range of backazimuths, and the measured null directions are consistent with the measured fast directions beneath the station. This behavior is characteristic of stations located in the southern part of the study area, where the splitting tends to be large ($\delta t = 1.5$ – 2.5 s) and the splitting patterns are simple and exhibit little spatial variation.

Fig. 7b shows a circular histogram of all fast direction measurements shown in Fig. 5a along with a histogram of the corresponding delay times. The circular histogram is overwhelmingly dominated by nearly E-W fast directions and the delay time measurements yield an average δt of ~ 1.8 s, with well-constrained δt values of up to ~ 3 s and a standard deviation of 0.49 s. This average delay time is considerably

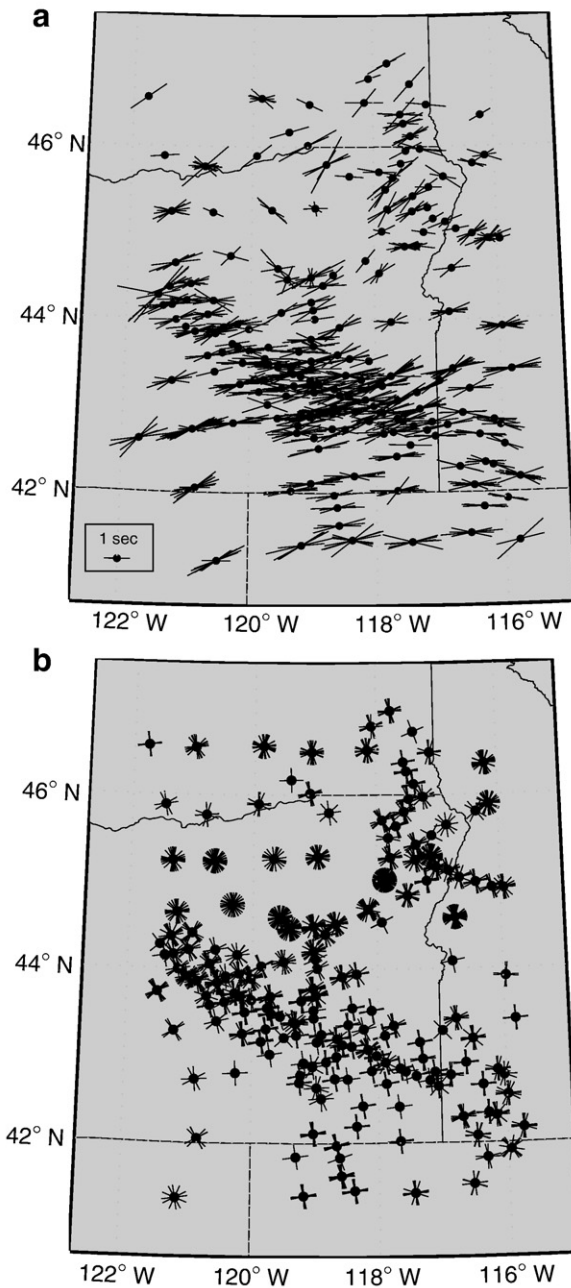


Fig. 5. a. Map of individual splitting measurements in the data set, plotted at the station location. The orientation and length of the bar correspond to the fast direction and delay time, respectively. For clarity, we have shown only the highest-quality measurements at each station; either all “good” measurements or, at stations where no “good” measurements were found, all “fair” measurements. b. Map of all “good” and “fair” quality null measurements, plotted at the station location as crosses whose bars correspond to the backazimuth of the event and the corresponding potential null direction. Many stations in the northern part of the study area exhibit null directions over a large range of backazimuths, indicating weak and/or complex anisotropy beneath the station.

higher than the global average of ~ 1 s for continental regions (e.g., Silver, 1996), which indicates that the anisotropy beneath eastern Oregon is unusually strong and/or that the anisotropic layer in the upper mantle is unusually thick.

In order to present a clear first-order picture of SKS splitting and mantle flow patterns beneath eastern Oregon, we calculate average splitting parameters (ϕ , δt) for each station in the data set (splitting parameter values can be found in the supplementary data). These single-station average splitting parameter estimates are, in general,

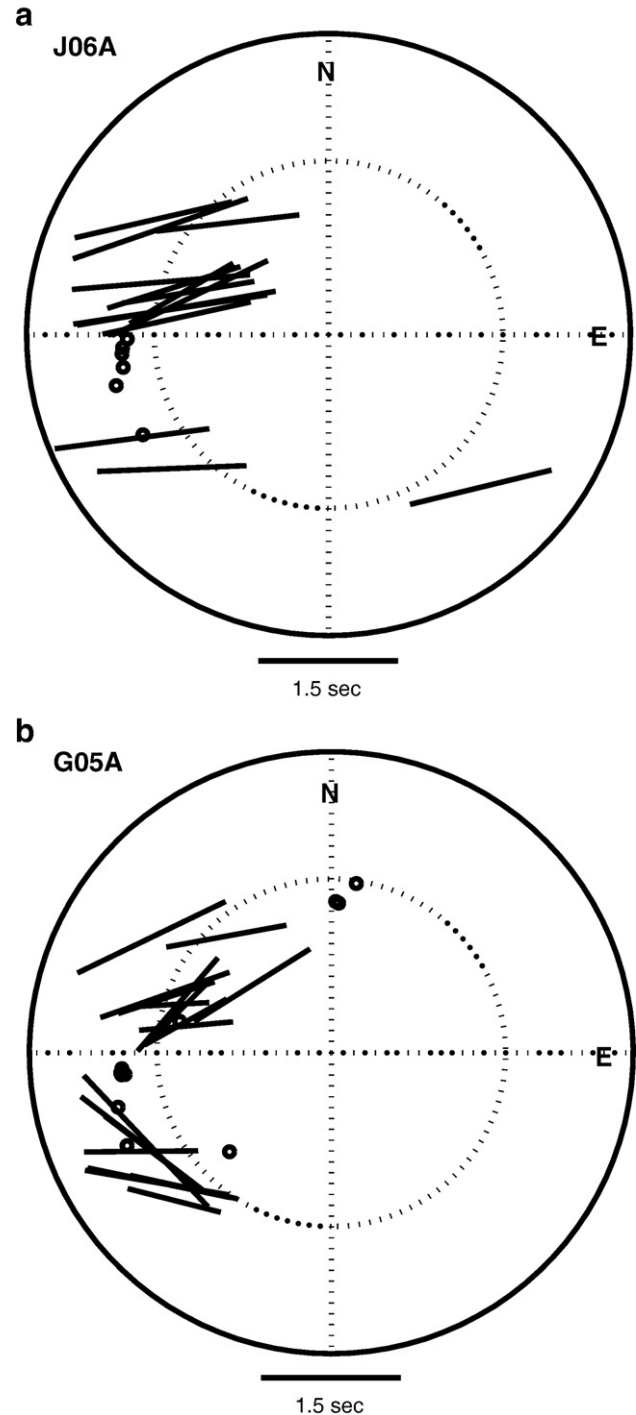


Fig. 6. Examples of detailed splitting patterns at two stations (J06A and G05A; station locations are shown in Fig. 2). Bars representing splitting parameters are plotted as a function of backazimuth and incidence angle (hatched line indicates an incidence angle of 8°). All “good” and “fair” measurements are shown (note that this is a larger subset of the measurements than shown in Fig. 5a, where only the “good” quality measurements are shown). Null measurements are plotted as circles. a. Splitting pattern observed at station J06A, located in the HLP. The splitting measurements exhibit very little variation with backazimuth. b. Splitting pattern observed at station G05A, located in the northern part of the study area. At this station the splitting pattern is markedly more complicated and the measured splitting parameters exhibit significant variation with backazimuth.

more reliable in the southern part of the study region where the splitting patterns are simpler. The map of average splitting parameters for each station is shown in Fig. 8, and there are a few regional trends that are evident from this map. First, there are clear trends in the distribution of average delay times, with the smallest average δt

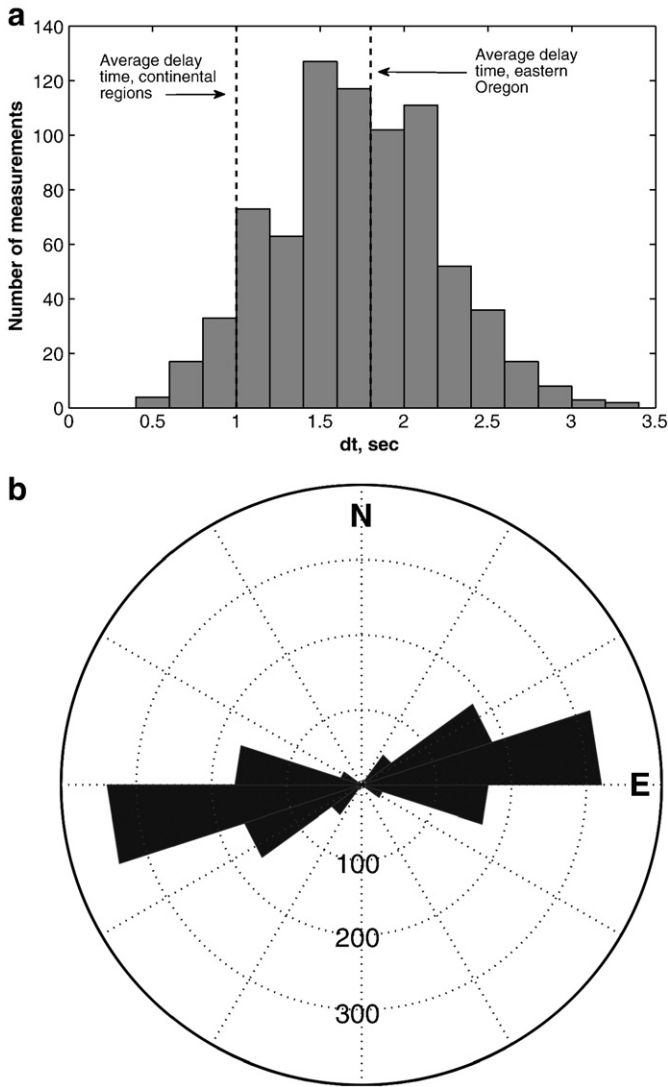


Fig. 7. a. Histogram of measured delay times shown in Fig. 5a. b. Circular histogram of measured fast directions shown in Fig. 5a.

values in the Wallowa Mountain region, and slightly larger δt at stations to the north of the Wallowas. Further to the south, delay times tend to be larger ($\delta t > 1.2$ s) and there is a concentration of still larger delay times ($\delta t > 1.7$ s) in the southeastern part of Oregon. The largest delay times ($\delta t > 2.2$ s) delineate a region in the heart of the HLP province (Fig. 8). There is also a small group of stations to the north of Newberry volcano that exhibit somewhat larger delay times than the surrounding stations. Spatial variations in the fast directions are more subtle, but there are a few well-defined patterns. In the HLP, most fast directions strike approximately N80°E, and although there are a few isolated regions that exhibit some complexity in ϕ , the overall pattern is remarkably uniform. In a few regions, including the Owyhee Plateau and stations located in the southwestern part of the study area, there is a slight rotation of the ϕ values; in the Owyhees, the average fast directions strike approximately N100°E, while stations in south-central Oregon and northern California tend to exhibit fast directions closer to ~N60°E. In northeastern Oregon and southeastern Washington, there is a slight rotation to more northeasterly fast directions, although the more complex splitting patterns observed in this region means that the single-station average splitting parameters may be less reliable than in the HLP.

The splitting pattern shown in Fig. 8 is consistent with results from previous studies of eastern Oregon splitting (e.g., Xue and Allen,

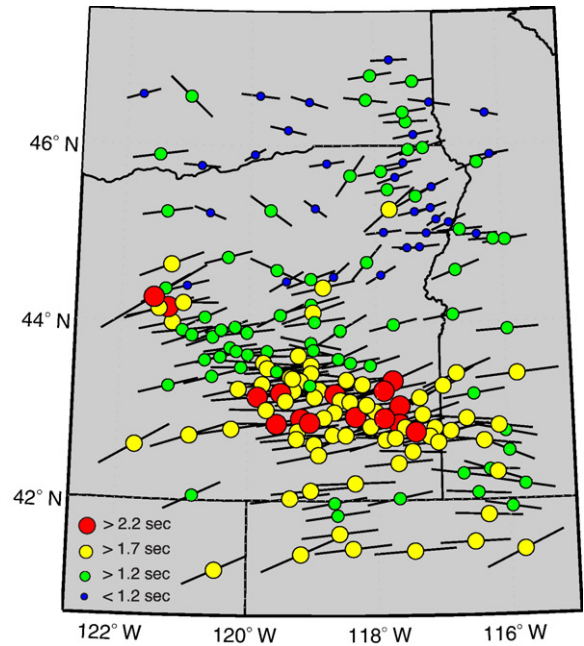


Fig. 8. Map of average splitting parameters in Eastern Oregon and surrounding regions. Estimates were obtained by a simple average of the highest-quality measurements at each station; nulls were not taken into account in the averaging process. The symbols are color-coded by the magnitude of the delay time, as indicated by the legend at bottom left, but the length of the bar is uniform at all stations.

2006), although the data set described here has much better spatial resolution than previous studies. The pattern in fast directions found in our study region is also generally consistent with the larger-scale splitting pattern observed in the western US (e.g., Zandt and Humphreys, 2008; Fouch and West, in preparation). We emphasize, however, that the High Lava Plains region of Oregon represents the broadest region of particularly high delay times in the western US (which is itself a region of relatively high δt compared to most continental regions). The high δt observed in the HLP contrast with those observed in the eastern Snake River Plain, which average ~1.0–1.5 s. This contrast is notable, as the eastern SRP is also associated with temporally migrating tectonomagmatic activity (with volcanic production that is an order of magnitude more voluminous than in the HLP).

5. Interpretation

5.1. Distinguishing between lithospheric and asthenospheric anisotropy

A first key question is whether the splitting observed in eastern Oregon reflects anisotropy in the crust, in the mantle lithosphere (reflecting past deformational episodes), in the asthenosphere (related to present-day mantle flow), or a combination of these factors. Because SKS paths through the upper mantle are nearly vertical, and because shear wave splitting is a path-integrated measurement, the depth resolution of the measurements is poor. However, an argument about the relative contribution from different parts of the crust/mantle system can be made based on the large delay times observed in this study and the likely thickness of the lithosphere in the region. In the HLP, the unusually large delay times argue for a primary contribution from the asthenospheric mantle. The lithosphere beneath the HLP is likely thin; S wave velocities in the uppermost mantle to depths of 50 km or even less are low (~4.2 km/s; Li et al., 2007; Warren et al., 2008) and the mantle lithosphere is considerably thinner here (~50–60 km thick) than in the cratonic

region to the east (e.g., Lowry and Smith, 1995). Because the observed delay times are so large, a model in which all of the anisotropy is in the crust and mantle lithosphere would imply an unreasonably large magnitude of anisotropy (roughly 20% anisotropy for a ~60 km thick lithosphere) and we can confidently infer that the large delay times and uniform fast directions reflect contemporary flow in the asthenospheric mantle. While a small contribution to the observed splitting from crustal anisotropy is likely, average values for crustal splitting are on the order of perhaps ~0.1–0.3 s (e.g., Savage, 1999) and thus the large delay times observed here cannot be attributed mainly to crustal anisotropy. Even if we attribute 1 s of delay time to anisotropy in the crust and mantle lithosphere, the asthenosphere would have to contribute 1.5–2 s of splitting beneath the central HLP, which corresponds to ~6–8% anisotropy for a 150-km thick asthenosphere. This is within the observed range for mantle-derived xenoliths (e.g., Mainprice and Silver, 1993; Ben Ismail and Mainprice, 1998).

At stations located in the northern part of our study area, most notably in the Blue and Wallowa Mountains, the relative contributions to the observed splitting from the crust, lithosphere, and asthenosphere are less clear-cut. The splitting in this region is often weaker than in the HLP and the lithosphere is likely to be thicker (e.g., Lowry and Smith, 1995; Roth et al., 2008). Splitting patterns at individual stations in this region are often complicated, which implies that the anisotropic structure beneath this region is complex. In particular, the observation of well-constrained null measurements over a wide range of backazimuths (Fig. 5b) indicates that the anisotropy in this region is weaker and more complex than beneath the HLP. This, in turn, indicates a likely contribution from several different regions of the crust and/or upper mantle; the complicated SKS waveforms and splitting patterns observed in the Wallowas are plausibly due to multiple layers of anisotropy, considerable lateral heterogeneity, vertical mantle flow (i.e., West et al., 2009), or a combination of these factors. Without more detailed modeling, it is difficult to characterize the relative contributions to the observed splitting from the lithospheric vs. asthenospheric upper mantle, but we can say with confidence that the lithosphere and/or crust likely makes a significant contribution to the splitting signal in this region, in marked contrast to the HLP. Despite the indications of complexity, however, the average fast directions for stations in the Wallowa array tend to be roughly E-W, as in the southern part of the study area.

5.2. Implications for mantle flow

In order to infer the flow direction beneath a seismic station from an observed fast splitting direction, knowledge of the relationship between strain and anisotropy is required. Our understanding of this relationship comes from mineral physics experiments and petrographic analysis of mantle-derived rocks (for recent overviews, see Karato et al. (2008) and Mainprice (2007)). The usual relationship used to interpret shear wave splitting beneath continents is that the fast splitting direction tends to align with the mantle flow direction beneath the station, based on experimental results from olivine aggregates deformed in simple shear that produce so-called A-type olivine fabric. Mineral physics studies have shown that this relationship can be affected by the physical conditions associated with deformation, including temperature, stress, water content, and pressure (e.g., Karato et al., 2008). It is generally thought that the conditions needed to produce B-type olivine fabric – a fabric which is rotated by 90° from the customary expected relationship between strain and anisotropy – are not present in the subcontinental asthenosphere (Karato et al., 2008). While some recent experiments have suggested that B-type fabric can be produced in the laboratory at pressures greater than ~3 GPa (corresponding to a mantle depth of ~100 km; Jung et al., 2009), the applicability of these experiments to mantle conditions remains uncertain (e.g., Long and Silver, 2009), and geodynamical modeling studies that utilize the A-type (or similar)

fabric paradigm to explain splitting patterns in the western United States have been quite successful (e.g., Silver and Holt, 2002; Becker et al., 2006). Therefore, we rely on the usual relationship used to interpret anisotropy beneath continents (see also Fouch and Rondenay, 2006) and infer that the fast splitting direction indicates the direction of (horizontal) mantle flow beneath the station.

The strong, consistent splitting with an E-W fast direction observed at stations in southeastern Oregon, western Idaho, and northern Nevada suggests the presence of a well-organized mantle flow field beneath the region. Because the splitting patterns observed in the HLP are generally simple and exhibit little backazimuthal variation that might indicate multiple anisotropic layers, and because the large delay times argue for a primary contribution from the asthenospheric mantle, their interpretation is much less ambiguous than is typical for shear wave splitting measurements in a continental setting. We argue that the strong E-W splitting observed beneath the HLP can be unambiguously attributed to consistent and well-organized flow in the asthenospheric upper mantle in a roughly E-W direction. This E-W direction does not align with either the strike of the HLP volcanic trend or with the direction of absolute plate motion (Fig. 1). In the northern part of our study area, it is more difficult to make a blanket statement about the direction of mantle flow, because the relative contributions to the splitting signal from frozen lithospheric anisotropy and active flow in the asthenosphere are more difficult to assess. One possibility is that the mantle flow direction beneath the Blue and Wallowa Mountains is similar to that beneath the HLP, but an additional contribution to splitting from the lithosphere and/or crust results in a complex splitting signal and reduced delay times. Without more detailed multiple-layer modeling of the splitting patterns observed in this region, however, it is not possible to characterize fully the active mantle flow regime.

5.3. The source of the large delay times

As the histogram in Fig. 7 demonstrates, the average delay times observed in eastern Oregon are considerably higher than the global average for continental regions, and in the heart of the HLP they range up to ~3 s, on the high end of the range of delay times observed globally for SKS-type phases (e.g., Fouch and Rondenay, 2006; Long and Silver, 2009). Understanding the source of these unusually large delay times is an important piece in sorting out the puzzle of the origin and evolution of the HLP. Strikingly, the magnitude of the delay times in eastern Oregon and the surrounding regions seem to correlate spatially with isotropic uppermost mantle wavespeeds inferred from body wave tomography (e.g., Roth et al., 2008; West et al., 2009). Specifically, relatively low wavespeeds and relatively high δt values are found beneath the HLP and in the vicinity of Newberry volcano, while relatively high wavespeeds and relatively low δt are found beneath the northern part of the study area, particularly the Blue and Wallowa Mountains (Fig. 9).

There are three possible scenarios that would result in unusually high delay times. First, the thickness of the anisotropic layer beneath the HLP might be greater than is usual for continental regions. Because the splitting is inferred to be due to the LPO of olivine in the asthenospheric mantle, it is plausible that the thin lithosphere beneath the HLP is associated with a correspondingly thick asthenosphere. It seems unlikely, however, that any difference in asthenospheric thickness could explain delay times of ~2.5–3.0 s instead of the typical ~1 s. A second possibility is that olivine LPO is particularly strong in the anisotropic layer beneath the HLP, possibly due to differences in upper mantle temperatures or due to local differences in water content. There is, however, little experimental data on the effect of temperature or other factors such as water content on the strength of LPO. The overall strength of LPO beneath the region may also be stronger than surrounding areas due simply to particularly well-organized and coherent mantle flow.

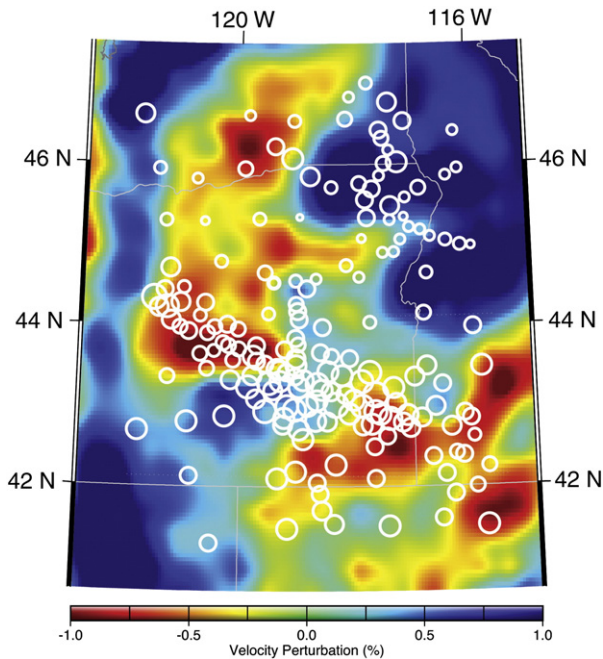


Fig. 9. A horizontal slice through the three-dimensional P velocity model of West et al. (2009) at a depth of 100 km. The single-station average delay times (see Fig. 8) are plotted at the station locations; the size of the circle corresponds to the size of the delay time, with the smallest circles corresponding to delay times < 0.6 s and the largest corresponding to delay times > 2.2 s. To first order, relatively fast uppermost mantle wavespeeds correlate spatially with relatively low splitting delay times and vice versa. This correlation is not perfect, however, particularly in the central part of the HLP, where splitting delay times are large but P wave velocities are not particularly low.

A third possibility is that there is an additional contribution to the observed splitting from the shape preferred orientation of partial melt in the uppermost mantle, which can result in strong anisotropy (e.g., Zimmerman et al., 1999). There is some indication that the largest delay times in the eastern Oregon data set are spatially correlated with Holocene volcanism; both Jordan Craters and Diamond Craters are located within the swath of particularly high delay times, and δt values at stations just to the north of Newberry are also higher than at surrounding stations (Figs. 2 and 8). Enhanced delay times due to a contribution from the shape preferred orientation of partial melt might plausibly explain the difference between the HLP and the Willowa Mountains, as one major difference between these regions is the probable presence or absence of partial melt. It has been shown that a small amount of partial melt (a few percent) can result in significant anisotropy if the melt is aligned in lenses or similar shapes (Vauchez et al., 2000), and a preexisting LPO may also play a role in aligning melt structures (Waff and Faul, 1992); the presence of partial melt may also, in turn, affect the development of olivine LPO (Holtzman et al., 2003). Partial melt has been invoked to explain large delay times observed in New Zealand (Greve et al., 2008; Greve and Savage, 2009), but because the relationships between mantle flow, the alignment of partial melt, and the resulting anisotropy remain poorly understood, it is difficult to quantitatively test the ability of partial melt to explain the eastern Oregon splitting patterns.

The shape preferred orientation of partial melt may play a role in generating the high delay times observed in this study, but there is no compelling evidence as yet that partial melt is ubiquitous in the upper mantle beneath the HLP, which would seem to be required to explain the widespread high δt values with a shape preferred orientation mechanism. A combination of the three mechanisms discussed here may be required to explain the large delay times observed in the HLP, but given the first-order spatial correlation between relatively slow upper mantle wavespeeds and high delay times, we cannot at present rule out any of the three mechanisms discussed here.

5.4. Explaining lateral variations in delay times in the HLP

The observation of splitting delay times within the HLP province that are both unusually large and that vary spatially over small length scales is one of the most intriguing findings of this study. Because the SKS waves under study have characteristic periods of ~ 10 s, their associated regions of sensitivity (which can be approximated by the first Fresnel zone) will be relatively large at depth (e.g., Long et al., 2008). The observation of small-scale variations in δt therefore suggests that the responsible spatial variations in anisotropy are likely to be relatively shallow, most likely in the uppermost mantle. The combination of unusually large δt and small-scale variations in δt values argues for an anisotropic model in which the geometry of the anisotropy varies little but the strength of the anisotropy exhibits strong lateral variations. In contrast, a model in which the geometry of anisotropy varied dramatically over small length scales would result in relatively small average delay times, as finite-frequency shear wave splitting measurements would tend to average over regions of incoherent anisotropic structure. While the dataset presented here does not uniquely constrain a mechanism for the lateral variations in delay times observed in the HLP, the enhanced delay times in the central HLP must be consistent with a mechanism (perhaps stronger LPO or partial melt) that is capable of producing lateral variations in the strength of anisotropy without corresponding variations in its geometry.

5.5. Implications for the tectonic evolution of eastern Oregon

As discussed in Section 5.2, the combination of large delay times and uniformly E-W fast directions beneath the HLP places a very strong constraint on the geometry of mantle flow in this region. In turn, this knowledge of the mantle flow patterns in the region places a strong constraint on models for the tectonic evolution of eastern Oregon. By itself, our inference of strong, coherent E-W mantle flow does not uniquely constrain such a model. However, any model proposed for the formation of the HLP and, more generally, for the volcanic history and tectonic evolution of eastern Oregon and the surrounding region must be consistent with the constraints on present-day mantle flow provided by the splitting observations. One possible mechanism for consistent E-W mantle flow beneath the HLP is that it is a consequence of the rollback of the Cascadia slab; the E-W direction is roughly parallel to the direction of present-day trench migration. Further to the north, the complexity in the splitting patterns may indicate a local disturbance to the large-scale E-W flow field near the edge of the North American craton.

We emphasize that models invoking a mantle plume to drive mantle flow in a pattern radiating out from the presumed plume impact location in southeastern Oregon (e.g., Camp and Ross, 2004) do not appear to be consistent with the upper mantle flow field inferred here. The splitting observations are not consistent with any model that requires mantle flow in a northwestern direction along the strike of the spatiotemporal trend in silicic volcanic activity in the HLP. This interpretation is consistent with the inferences from the tomographic wavespeed models of Roth et al. (2008) and the Rayleigh wave dispersion analysis of Warren et al. (2008) that the presence of a plume beneath the HLP volcanic province is not required by seismic data.

6. Outlook and summary

The splitting data set presented here provides a first-order picture of anisotropy and deformation in the upper mantle beneath eastern Oregon and yields strong constraints on the contemporary flow geometry in the asthenosphere. Work on characterizing the detailed anisotropic structure (and the tectonic processes that generate it) of the crust/mantle lithosphere/asthenosphere system beneath eastern

Oregon continues. In particular, an additional year of data from the HLP experiment (Fall 2008–Fall 2009) will shortly be available. This will allow us to characterize splitting patterns at individual stations in greater detail with regard to potential backazimuthal complexity that might indicate complex anisotropy, particularly if splitting measurements from direct teleseismic S phases are included. For stations located farther to the north in the Blue and Wallowa regions, where the splitting patterns are consistent with complex anisotropy beneath the stations and may reflect contributions from both lithospheric and asthenospheric structure, a forward modeling approach that takes into account multiple layers of anisotropy should further constrain anisotropic structure at depth. The measurement of splitting parameters over a range of frequency bands may also shed additional light on complex anisotropy, as splitting has been shown to be frequency dependent in the presence of complex structure (e.g., Marson-Pidgeon and Savage, 1997; Fouch and Fischer, 1998) and high-frequency measurements may be biased towards near-surface anisotropy (e.g., Saltzer et al., 2000).

The data set presented here, with its excellent spatial resolution, is also a very promising candidate for the application of new methods for shear wave splitting tomography to image anisotropic structure at depth (e.g., Chevrot, 2006; Long et al., 2008). The tomographic inversion of measurements of the splitting intensity, a quantity that is closely related to the splitting parameters (ϕ , δt) measured in this study, can resolve the 2-D or 3-D distribution of anisotropy at depth and, in particular, can place constraints on the depth distribution of anisotropy. Another promising line of inquiry is the integration of the shear wave splitting measurements presented here with a geodynamical modeling framework to help to narrow the class of plausible models for mantle dynamics beneath eastern Oregon. Laboratory models that take into account the kinematics and temporal evolution of the Juan de Fuca slab, the possible effects of a plume, and the effects of lithospheric topography on the resulting mantle flow field have been carried out (e.g., Kincaid et al., 2008) and we are currently comparing splitting predictions from these models to the dataset presented in this paper. Such detailed comparisons will provide strong constraints on the type of models that are consistent with the splitting observations. Finally, we expect to integrate the SKS splitting measurements with other constraints on anisotropy, including measurements of direction-dependent Pn (and possibly Sn) velocities from the active source component of the HLP project and constraints on azimuthal anisotropy from surface wave inversions. In particular, constraints on the magnitude of anisotropy in the uppermost mantle from Pn measurements may in turn constrain a possible contribution to splitting from the shape preferred orientation of partial melt in the shallowest mantle.

To summarize, the shear wave splitting trends in eastern Oregon are fairly simple and tend to be dominated by approximately E-W fast directions and delay times that range from ~0.8 s to ~2.7 s. We observe a difference in splitting patterns between stations located in southeastern Oregon and stations located further to the north in northeastern Oregon and southern Washington. At stations located in the Blue and Wallowa Mountain regions, the splitting patterns tend to be complex at individual stations, exhibiting well-constrained null measurements over a wide range of backazimuths and smaller delay times than the rest of the study region. We interpret this as evidence for weaker and/or more complex azimuthal anisotropy, suggesting that SKS splitting in this region reflects contributions from both active mantle flow in the asthenosphere and frozen lithospheric anisotropy. In the HLP, the splitting patterns are simpler than those observed farther to the north; fast directions are predominantly E-W, ranging from ~N80°E to ~N100°W. Delay times in the HLP are large, with an average value of ~1.8 s and maximum values of ~2.7 s at individual stations. The observed splitting cannot be primarily due to relict anisotropy in the lithosphere and likely reflects contemporary mantle flow beneath the HLP in a generally E-W direction. The largest delay

times observed in the HLP correlate spatially with regions of slow isotropic mantle wavespeeds and with the occurrence of Holocene volcanism. The large HLP delay times could be a consequence of a thicker-than-average anisotropic layer beneath the region, particularly strong LPO, a contribution to anisotropy from the shape preferred orientation of melt, or a combination of these processes. The splitting measurements presented here place a very strong constraint on present-day mantle flow beneath eastern Oregon, particularly beneath the HLP, and any model for the recent tectonic evolution and volcanic activity of this region must be consistent with the generally E-W mantle flow that is inferred from the SKS splitting measurements.

Acknowledgements

Data from the USArray Transportable Array, High Lava Plains, and Wallowa Mountains deployments were used in this study and we thank the vast network of people involved in making these experiments a success. In particular, we thank the staff members at the IRIS PASSCAL and DMC facilities and the USArray TA operations staff who have done so much to make these experiments happen and to make the data accessible. Major contributions to the success of the HLP deployment have been made by Jenda Johnson, Steven Golden, the Eastern Oregon Agricultural Research Center, the many landowners who hosted HLP stations, and the many students, postdocs, and volunteers who helped with the fieldwork effort. We are grateful to the PIs, postdocs, and students involved with the HLP project (www.dtm.ciw.edu/research/HLP) for stimulating scientific discussions, particularly Rick Carlson, Chris Kincaid, and Kelsey Druken. We thank David Abt, Martha Savage, and an anonymous reviewer for their thoughtful and helpful reviews. The High Lava Plains experiment is funded by the National Science Foundation (NSF) through awards EAR-0507248 (MJF) and EAR-0506914 (DEJ). The Wallowa Mountains experiment is funded through NSF award EAR-051000 (EH). AK's participation was supported through the Carnegie Institution of Washington Summer Intern Program in Geoscience, which is funded by NSF-EAR through the Research Experiences for Undergraduates program.

Appendix A. Supplementary data

Supplementary data associated with this article can be found in the online version. doi:10.1016/j.epsl.2009.09.039

References

- Becker, T.W., Schulte-Pelkum, V., Blackman, D.K., Kellogg, J.B., O'Connell, R.J., 2006. Mantle flow under the western United States from shear wave splitting. *Earth Planet. Sci. Lett.* 247, 235–251.
- Ben Ismail, W., Mainprice, D., 1998. A statistical view of the strength of seismic anisotropy in the upper mantle based on petrofabric studies of ophiolite and xenolith samples. *Tectonophysics* 296, 145–157.
- Burdick, S., Li, C., Martynov, V., Cox, T., Eakins, J., Multer, T., Astiz, L., Vernon, F.L., Pavlis, G.L., van der Hilst, R.D., 2008. Upper mantle heterogeneity beneath North America from travel time tomography with global and USArray Transportable Array data. *Seismol. Res. Lett.* 79, 384–387.
- Camp, V.E., Ross, M.E., 2004. Mantle dynamics and genesis of mafic magmatism in the intermontane Pacific Northwest. *J. Geophys. Res.* 109, B08204. doi:10.1029/2003JB002838.
- Carlson, R.W., Hart, W.K., 1987. Crustal genesis on the Oregon Plateau. *J. Geophys. Res.* 92, 6191–6206.
- Chevrot, S., 2006. Finite-frequency vectorial tomography: a new method for high-resolution imaging of upper mantle anisotropy. *Geophys. J. Int.* 165, 641–657.
- Christiansen, R.L., McKee, E.H., 1978. Late Cenozoic volcanic and tectonic evolution of the Great Basin and Columbia inter-montane regions. *Geol. Soc. Am. Mem.* 152, 283–311.
- Christiansen, R.L., Foulger, G.R., Evans, J.R., 2002. Upper mantle origin of the Yellowstone hot spot. *Geol. Soc. Am. Bull.* 114, 1245–1256.
- Cross, T.A., Pilger, R.H., 1978. Constraints on absolute motion and plate interaction inferred from Cenozoic igneous activity in the western United States. *Am. J. Sci.* 278, 865–902.

- Fouch, M.J., Fischer, K.M., 1998. Shear wave anisotropy in the Mariana subduction zone. *Geophys. Res. Lett.* 25, 1221–1224.
- Fouch, M.J., Rondenay, S., 2006. Seismic anisotropy beneath stable continental interiors. *Phys. Earth Planet. Inter.* 158, 292–320.
- Fouch, M.J., West, J.D., in preparation. The mantle flow field beneath western North America.
- Greve, S.M., Savage, M.K., 2009. Modelling seismic anisotropy variations across the Hikurangi subduction margin. *New Zealand Earth Planet. Sci. Lett.* 285, 16–26.
- Greve, S.M., Savage, M.K., Hoffman, S.D., 2008. Strong variations in seismic anisotropy across the Hikurangi subduction zone, North Island, New Zealand. *Tectonophysics* 462, 7–21.
- Hales, T.C., Abt, D.L., Humphreys, E.D., Roering, J.J., 2005. A lithospheric instability origin for Columbia River flood basalts and Wallowa Mountains uplift in northeast Oregon. *Nature* 438, 842–845.
- Holtzman, B., Kohlstedt, D.L., Zimmerman, M.E., Heidelbach, F., Hiraga, T., Hustoft, J., 2003. Melt segregation and strain partitioning: implications for seismic anisotropy and mantle flow. *Science* 301, 1227–1230.
- Hooper, P.R., Camp, V.E., Reidel, S.P., Ross, M.E., 2007. The origin of the Columbia River flood basalt province: plume versus nonplume models. In: Foulger, G.R., Jurdy, D.M. (Eds.), *Plates, plumes, and planetary processes: Geol. Soc. Am. Special Paper*, vol. 430, pp. 635–668.
- Humphreys, E.D., Coblenz, D.D., 2007. North American dynamics and western U.S. tectonics. *Rev. Geophys.* 45. doi:10.1029/2005RG000181.
- Humphreys, E.D., Deuker, K.G., Schutt, D.L., Smith, R.B., 2000. Beneath Yellowstone: evaluating plume and nonplume models using teleseismic images of the upper mantle. *GSA Today* 10, 1–7.
- Jordan, B.T., 2005. Age-progressive volcanism of the Oregon High Lava Plains: overview and evaluation of tectonic models. In: Foulger, G.R., et al. (Ed.), *Plates, Plumes, and Paradigms: Geological Society of America Memoir*, vol. 388, pp. 503–515.
- Jordan, B.T., Grunder, A.L., Duncan, R.A., Deino, A.L., 2004. Geochronology of age-progressive volcanism of the Oregon High Lava Plains: implications for the plume interpretation of Yellowstone. *J. Geophys. Res.* 109, B10202. doi:10.1029/2003JB002776.
- Jung, H., Mo, W., Green, H.W., 2009. Upper mantle seismic anisotropy resulting from pressure-induced slip transition in olivine. *Nature Geosci.* 2, 73–77.
- Karato, S., Jung, H., Katayama, I., Skemer, P., 2008. Geodynamic significance of seismic anisotropy of the upper mantle: new insights from laboratory studies. *Annu. Rev. Earth Planet. Sci.* 36, 59–95.
- Kincaid, C., Druken, K., Griffiths, R., 2008. Laboratory models of three-dimensional mantle flow and plume dispersion driven by rollback subduction and back-arc extension. *International Geological Congress*, Oslo, Norway.
- Leeman, W.P., Oldow, J.S., Hart, W.K., 1992. Lithosphere-scale thrusting in the western U.S. Cordillera as constrained by Sr and Nd isotopic transitions in Neogene volcanic rocks. *Geology* 20, 63–66.
- Li, X., Yuan, X., Kind, R., 2007. The lithosphere-asthenosphere boundary beneath the western United States. *Geophys. J. Int.* 170, 700–710.
- Lipman, P.W., Prostka, H.J., Christensen, R.L., 1972. Cenozoic volcanism and plate tectonic evolution of the western United States. *I. Phil. Trans. Roy. Soc. London, Ser. A* 271, 217–248.
- Long, M.D., Silver, P.G., 2009. Shear wave splitting and mantle anisotropy: measurements, interpretations, and new directions. *Surv. Geophys.* 30, 407–461.
- Long, M.D., van der Hilst, R.D., 2005. Estimating shear wave splitting parameters from broadband recordings in Japan: a comparison of three methods. *Bull. Seismol. Soc. Am.* 95, 1346–1358.
- Long, M.D., de Hoop, M.V., van der Hilst, R.D., 2008. Wave-equation shear wave splitting tomography. *Geophys. J. Int.* 172, 311–330.
- Lowry, A.R., Smith, R.B., 1995. Strength and rheology of the western U.S. Cordillera. *J. Geophys. Res.* 100, 17,947–17,963.
- Mainprice, D., 2007. Seismic anisotropy of the deep Earth from a mineral and rock physics perspective. In: Schubert, G. (Ed.), *Treatise on Geophysics* v. 2, pp. 437–492.
- Mainprice, D., Silver, P.G., 1993. Interpretation of SKS waves using samples from the subcontinental lithosphere. *Phys. Earth Planet. Inter.* 78, 257–280.
- Marson-Pidgeon, K., Savage, M.K., 1997. Frequency-dependent anisotropy in Wellington, New Zealand. *Geophys. Res. Lett.* 24, 3297–3300.
- McCaffrey, R., Long, M.D., Goldfinger, C., Zwick, P.C., Nabelek, J.L., Johnson, C.K., Smith, C., 2000. Rotation and plate locking at the southern Cascadia subduction zone. *Geophys. Res. Lett.* 27, 3117–3120.
- McCaffrey, R., Qamar, A.I., King, R.W., Wells, R., Khazaradze, G., Williams, C.A., Stevens, C.W., Vollick, J.J., Zwick, P.C., 2007. Fault locking, block rotation and crustal deformation in the Pacific Northwest. *Geophys. J. Int.* 169, 1315–1340.
- Pierce, K.L., Morgan, L.A., 1992. The track of the Yellowstone hot spot: volcanism, faulting, and uplift. In: Link, K., Kuntz, M.A., Platt, L.B. (Eds.), *Regional Geology of Eastern Idaho and Western Wyoming: Mem. Geol. Soc. Am.*, vol. 179, pp. 1–53.
- Roth, J.B., Fouch, M.J., James, D.E., Carlson, R.W., 2008. Three-dimensional seismic velocity structure of the northwestern United States. *Geophys. Res. Lett.* 35, L15304. doi:10.1029/2008GL034669.
- Saltzer, R.L., Gaherty, J., Jordan, T.H., 2000. How are vertical shear wave splitting measurement affected by variations in the orientation of azimuthal anisotropy with depth? *Geophys. J. Int.* 141, 374–390.
- Savage, M.K., 1999. Seismic anisotropy and mantle deformation: what have we learned from shear wave splitting? *Rev. Geophys.* 37, 65–106.
- Schellart, W.P., Stegman, D.R., Freeman, J., 2008. Global trench migration velocities and slab migration induced upper mantle volume fluxes: constraints to find an Earth reference frame based on minimizing viscous dissipation. *Earth-Science Rev.* 88, 118–144.
- Sigloch, K., McQuarrie, N., Nolet, G., 2008. Two-stage subduction history under North America inferred from multiple-frequency tomography. *Nature Geosci.* 1, 458–462.
- Silver, P.G., 1996. Seismic anisotropy beneath the continents: probing the depths of geology. *Annu. Rev. Earth Planet. Sci.* 24, 385–432.
- Silver, P.G., Chan, W.W., 1991. Shear wave splitting and subcontinental mantle deformation. *J. Geophys. Res.* 96, 16,429–16,454.
- Silver, P.G., Holt, W.E., 2002. The mantle flow field beneath western North America. *Science* 295, 1054–1057.
- Silver, P.G., Savage, M.K., 1994. The interpretation of shear-wave splitting parameters in the presence of two anisotropic layers. *Geophys. J. Int.* 119, 949–963.
- Smith, A.D., 1992. Back-arc convection model for Columbia River Basalt genesis. *Tectonophysics* 207, 269–285.
- Vauchez, A., Tommasi, A., Barruol, G., Maumus, J., 2000. Upper mantle deformation and seismic anisotropy in continental rifts. *Phys. Chem. Earth (A)* 25, 111–117.
- Waff, H.S., Faul, U.H., 1992. Effects of crystalline anisotropy on fluid distribution in ultramafic partial melts. *J. Geophys. Res.* 97, 9003–9014.
- Warren, L.M., Snoko, J.A., James, D.E., 2008. S-wave velocity structure beneath the High Lava Plains, Oregon, from Rayleigh-wave dispersion inversion. *Earth Planet. Sci. Lett.* 274, 121–131.
- Wernicke, B., Axen, G.J., Snow, J.K., 1988. Basin and Range extensional tectonics at the latitude of Las Vegas, Nevada. *Geol. Soc. Am. Bull.* 100, 1738–1757.
- West, J.D., Fouch, M.J., Roth, J.B., Elkins-Tanton, L.T., 2009. Seismic detection of vertical mantle flow from a lithospheric drip. *Nature Geosci.* 2, 439–444.
- Wüstefeld, A., Bokelmann, G., 2007. Null detection in shear-wave splitting measurements. *Bull. Seismol. Soc. Am.* 97, 1204–1211.
- Wüstefeld, A., Bokelmann, G., Barruol, G., Zaro, C., 2007. Splitlab: a shear-wave splitting environment in Matlab. *Comput. Geosci.* 34, 515–528.
- Xue, M., Allen, R.M., 2006. Origin of the Newberry hotspot track: evidence from shear-wave splitting. *Earth Planet. Sci. Lett.* 244, 315–322.
- Zandt, G., Humphreys, E., 2008. Toroidal mantle flow through the western U.S. slab window. *Geology* 36, 295–298.
- Zimmerman, M.E., Zhang, S., Kohlstedt, D.L., Karato, S., 1999. Melt distribution in mantle rocks deformed in simple shear. *Geophys. Res. Lett.* 26, 1505–1508.